Chapter 8
Cutting Force Estimation in Sensor-Equipped Metal Cutting Tools Using Strain-Force Transfer Function

Wu Peng, Anders Liljerehn, Martin Magnevall, and Dan Östling

Abstract Sensor-equipped cutting tools are becoming more common in the metal cutting industry as the demand for process monitoring and automation grows. These products are used for monitoring cutting forces and vibrations during machining with the objective of providing valuable insight into tool deflection, tool wear, surface finish, and process stability. The number of sensors and their position in the cutting tool, are often restricted by price and the thermo-mechanical loads acting in the cutting zone. Obtaining accurate measurements is a challenge due to mechanical filtering between the sensor positions and the tool tip as well as due to measurement noise from the sensors and electronics. This paper presents a method to estimate dynamic loads and tool tip vibrations using recorded data from strain sensors in a cutting tool. This is achieved through output-only calibration of an analytical model of the cutting tool, which defines the strain-force relationship based solely on the measured strain response data. This approach provides key parameters, including the first resonance frequency and the damping ratio of the cutting tool. The model is then applied to eliminate unwanted dynamic effects from the measured strain data, enhancing the accuracy of predictions of forces and tool tip displacement.

Keywords Cutting force estimation · Deflection prediction · Metal cutting dynamics · Sensor-equipped cutting tools · Strain-force transfer function

Introduction

As the demand for process monitoring and automation grows, sensor-equipped cutting tools are becoming increasingly common in the metal cutting industry [1]. This concept concerns expansion of existing products by adding sensors and communication devices on the tool body. Typically, two types of sensors are integrated: accelerometers, which measure vibration levels during machining, and strain sensors, which capture strain data used to estimate the deflection at the cutting tool tip. Measured data through these sensors provides the important insight into monitoring in-process conditions in terms of tool wear, surface finish and cutting process stability [2].

The machining process creates intense pressure and temperatures in the cutting zone, requiring sensors to be placed at a distance from the tool tip [3], as shown in Figure 1. This presents a challenge for accelerometers, which are ideally positioned as close to the tool tip as possible, where vibration amplitude is greatest. If not, accurately monitoring the vibration at the tool tip becomes difficult [4]. Another issue in these applications is signal distortion, caused by mechanical filtering through the transfer path [5, 6]. This means that the vibration transmitted from the tool tip to the sensor is affected by the dynamic properties of the tool body [7]. The conventional static calibration of strain sensor is hence insufficient to predict the dynamic loads acting at the tool tip. This is exemplified in Figure 2, where a statically calibrated strain sensor is used to predict the dynamic forces acting on the tool tip generated by a shaker and compared to the measurements from a laboratory-grade force sensor. The prediction of dynamic force at very low frequencies is accurate, but amplitude and phase deviations occur

Wu Peng · Anders Liljerehn
Department of Cutting Tool Research, AB Sandvik Coromant, Sandviken, SE 81181
e-mail: wu.peng@sandvik.com; anders.c.liljerehn@sandvik.com

Wu Peng · Martin Magnevall
Department of Mechanical Engineering, Blekinge Institute of Technology, Karlskrona, SE 37179
e-mail: wu.peng@sandvik.com; martin.magnevall@bth.se

Dan Östling
Department of Damped Solutions, Sandvik Teeness AS, Trondheim, NO 7053
e-mail: dan.ostling@sandvik.com

Walter D'Ambrogio, et al. (eds.), *Dynamic Substructuring & Transfer Path Analysis, Vol. 4*, Conference Proceedings of the Society for Experimental Mechanics Series, https://doi.org/10.13052/97887-438-0149-8_8

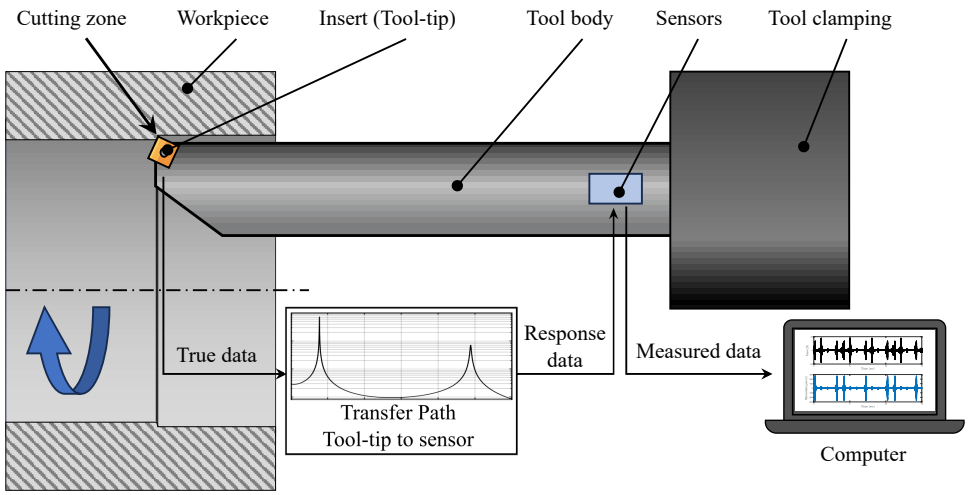

Fig. 1 An illustration of the information gets distorted between tool tip and sensor location on a sensor-equipped cutting tool in a cutting process.

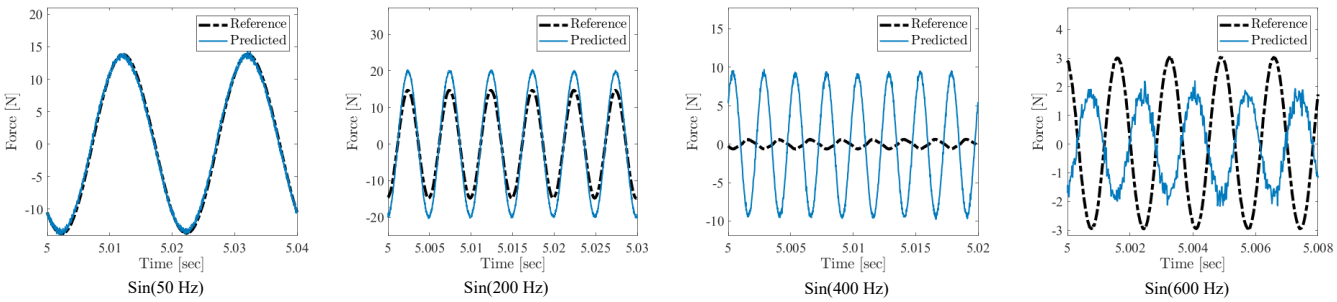

Fig. 2 Dynamic loads acting on the tool tip predictions using statically calibrated strain sensor on the cutting tool.

at higher frequencies. This issue presents a challenge in estimating not only the force but also the deflection at the tool tip using data from the strain sensor.

Several studies has been made on strain gauge-based dynamometer design for cutting force measurements. For example, Süleyman and Faruk [8] used octagonal rings to develop strain gauge based dynamometer for turning tool, maximizing sensitivity and minimizing cross-sensitivity to reduce the effect of the mechanical transfer path. This method has been proven to work under certain condition but there still remains challenges in measuring cutting forces with high accuracy. Östling et al. [9] presented a sensor-equipped boring bar to detect vibration level and cutting forces in turning process. This sensor-equipped tool uses strain gauges to measure static forces but does not take into account the mechanical transfer path necessary to estimate the cutting forces at higher frequencies.

This study evaluates the method presented in [10], where force estimations were performed on a cantilever beam equipped with a strain sensor. In this case, the study is extended to consider a physical cutting tool, assessing the method's ability to predict transient loads and, additionally, to estimate tool deflection. A novel aspect of this research is that model calibration is conducted solely on output data recorded from a strain sensor mounted on the cutting tool. This is accomplished by first creating an analytical model representation of the cutting tool describing the strain-force relationship. The model of strain-force transfer function is used to remove unwanted dynamic effects of the transfer path from the measured strain data to improve the estimation of the forces acting on the cutting tool. The estimated force is used as the input of conventional displacement-force transfer function to estimate the displacement response at the tool tip. The model representation requires calibration to ensure accurate predictions. This is challenging to performer by the end user of the tools where access to modal hammers or shaker equipment is limited. The paper hence evaluates the possibility to calibrate the model using response data only. This strategy would allow for calibration by simply exciting the system without recording the input force.

For reference evaluation, a direct drive-point frequency response function (FRF) is obtained using the measured input force and the accelerometer response at the tool tip. The accelerance frequency response is recalculated to displacement,

after which a state-space system identification scheme is applied to the displacement frequency response function, allowing for a direct estimation of the displacement response from the measured force data.

Method

This study investigates the single-direction vibration of a cutting tool equipped with a strain sensor near the clamping fixture, see Figure 3. The tool's specifications are detailed in Table 1. To estimate the force acting on the tool tip using the strain response from the sensor-equipped cutting tool, an analytical model is used to describe the strain-force relationship [10].

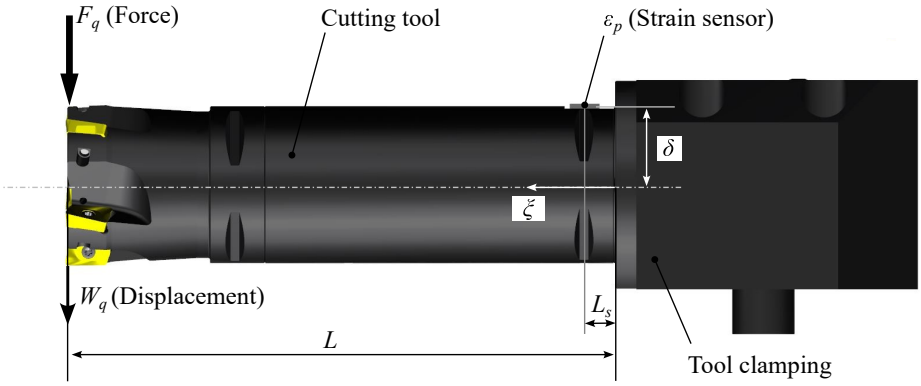

Fig. 3 An illustration of cutting tool (R390-066C6-18M060) with the extension adapter (C6-391.01-63 140A) and tool clamping (C6-RC2090-42060), equipped with a piezoelectric strain sensor.

Table 1 Specification of sensor-equipped cutting tool.

	Parameter	unit
Mass, m	5.515	kg
Length, L	203	mm
Diameter	63	mm
Distance from neutral axis, δ	31	mm
Sensor position, L_s	14	mm
Density, ρ	7850	$[kg/m^3]$
Young's modulus, E	206×10^9	$[Pa]$

The proposed methodology begins with an initial calibration stage Figure 4a, where the structure is excited, and the strain response, ϵ_p, is measured. From the measured strain the first resonance frequency, ω_{m1} and associated damping, ζ_1 are calculated. These extracted parameters are then used to update the analytical model, enabling the derivation of a calibrated representation of the strain-force transfer function, $H^{\epsilon}_{pq}(z)$, the inverse strain-force transfer function, $(H^{\epsilon}_{pq}(z))^{-1}$ and a displacement-force transfer function, $H^{d}_{qq}(z)$.

When the analytical model have been calibrated, the following steps are taken to complete the predictions for force and displacement: First, the strain response from the operational excitation force, F_o, is combined with the inverted strain-force transfer function, $(H^{\epsilon}_{pq}(z))^{-1}$ to calculate the predicted excitation force, F_q. Subsequently, the predicted displacement, W_q, can be derived from the predicted force using the displacement-force transfer function. A schematic diagram illustrating these steps is presented in Figure 4b.

The cutting tool is modeled as a cantilever beam, and the strain-force transfer function is described by its superposition residues, $\mathbb{R}^{\epsilon}_{pqr}$, and poles, λ_{pqr}, as:

$$H^{\epsilon}_{pq}(s) = \frac{\epsilon_p(s)}{F_q(s)} = \sum_{r=1}^{Nr} \frac{\mathbb{R}^{\epsilon}_{pqr}}{s-\lambda_r} + \frac{\mathbb{R}^{\epsilon *}_{pqr}}{s-\lambda^*_r} \tag{1}$$

where ϵ_p and F_q refers to the strain and force data with subscripts p and q being the response and excitation points. Nr refers to the total number of modes included, and s is the Laplace variable. Evaluating equation 1 along the $j\omega$ axis, the residues

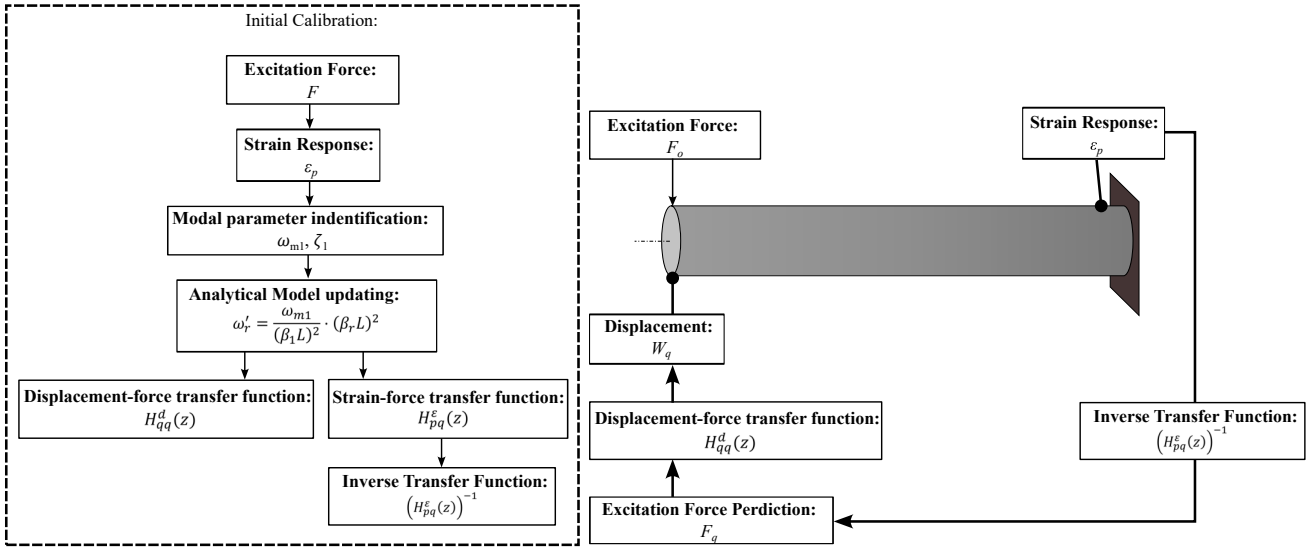

Fig. 4 (a): initial calibration steps for analytical model. (b):A schematic diagram of the method for estimating the force acting on the tool tip using the strain response of the cutting tool.

and poles can be expressed as:

$$\mathbb{R}_{pqr}^{\epsilon}, \mathbb{R}_{pqr}^{\epsilon *} = \mp j \frac{\phi_{pr}^{\epsilon}(\xi_p) \cdot \phi_{qr}(\xi_q)}{2\omega_{dr} m_r} \tag{2}$$

$$\lambda_{pqr}, \lambda_{pqr}^{*} = -\zeta_r \omega_r \pm j\omega_r \sqrt{1-\zeta_r^2} = -\zeta_r \omega_r \pm j\omega_{dr} \tag{3}$$

$$\omega_r = (\beta_r L)^2 \sqrt{\frac{EI}{mL^3}} \tag{4}$$

$$\phi_{qr}(\xi_q) = C_1 \cos(\beta_r \xi_q) + C_2 \sin(\beta_r \xi_q) + C_3 \cosh(\beta_r \xi_q) + C_4 \sinh(\beta_r \xi_q) \tag{5}$$

$$\phi_{pr}^{\epsilon}(\xi_p) = \delta \beta_r^2 \left[C_1 \cos(\beta_r \xi_p) + C_2 \sin(\beta_r \xi_p) - C_3 \cosh(\beta_r \xi_p) - C_4 \sinh(\beta_r \xi_p)\right] \tag{6}$$

where ϕ_{pr}^{ϵ} and ϕ_{qr} refer to the individual mode shapes at the response and excitation points. ω_{dr} refers to the damped resonance frequency of the mode r obtained from the poles and damping ratio ζ_r. ω_r refers to the undamped resonance frequency and β_r is the roots of the Euler-Bernoulli cantilever beam motion equation [11]. In equation 2, modal mass m_r of the beam is a measure of amount of mass moving in the given mode r. The modal mass of the beam can be calculated by equation 7, as presented in [12].

$$m_r = \int_0^L m_\rho \cdot |\phi_r(\xi)|^2 d\xi \tag{7}$$

The strain-force transfer function created in equation 1 need to be calibrated in order to accurately capture the boundary conditions in a real setup. The boundary conditions are typically more flexible than the idealized fixed conditions assumed in the analytical model. As a result, the resonance frequencies and peak values of the transfer function calculated from the model do not match those of the measured transfer function. To improve accuracy, the model is adapted to the cutting tool configuration based on the impulse strain response recorded from the strain sensor. This is achieved by applying a Fourier transform to this strain data allows the first resonance frequency ω_{m1} of the cutting tool to be obtained. To determine the damping ratio ζ_r of the cutting tool, logarithmic decrement approach is utilized [13, 14]. Figure 5 illustrates that logarithmic decrement relates the damping ratio to the strain response peaks through equation 8.

$$\zeta_r(\delta_N, N) = \frac{\delta_N/(2\pi N)}{\sqrt{1+(\delta_N/(2\pi N))^2}} \tag{8}$$

where the logarithmic decrement is defined as:

$$\delta_N = \ln\left(\frac{\mu\epsilon_1}{\mu\epsilon_N}\right) \tag{9}$$

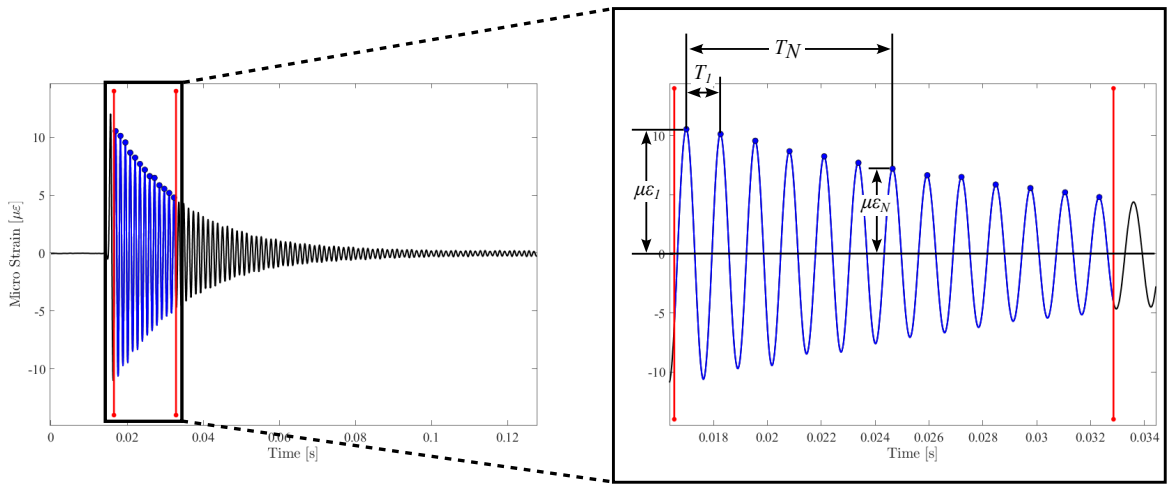

Fig. 5 An example of the measurement of impulse strain response recorded from sensor-equipped cutting tool taken in a logarithmic decrement analysis. In this case the period T_N is six times the damped period T_1, so $N = 6$.

Using the first resonance frequency ω_{m1} along with the equation 4, the resonance frequency of the first mode can be updated and the rest will follow through equation 10. The peaks values at each resonance frequency of the transfer function can be corrected by determined damping ratio ζ_r.

$$\omega_r^{'} = \frac{\omega_{m1}}{(\beta_1 L)^2} \cdot (\beta_r L)^2 \tag{10}$$

To effectively perform calculations using sampled strain data from the sensor, the transfer function must be converted into the discrete-time domain using the digital filter form of the equation 11 [15].

$$H^{\epsilon}(z) = \frac{B(z)}{A(z)} = \frac{\sum_{k=0}^{n_b} b(k) z^{-k}}{1 + \sum_{k=1}^{n_a} a(k) z^{-k}} = b(0) \frac{\prod_{k=1}^{n_b} (1 - Z_k z^{-1})}{\prod_{k=1}^{n_a} (1 - P_k z^{-1})} \tag{11}$$

where $b(k)$ and $a(k)$ are the coefficients of the numerator and denominator polynomials for the filter, while n_b and n_a denote the total number of coefficients. The roots of the numerator polynomial, Z_k, correspond to the zeros of the filter, while the roots of the denominator polynomial, P_k, are the poles. The selection of n_b and n_a is performed by visual inspection to ensure a satisfactory fit between the original transfer function and its filter representation.

To estimate forces from strain response data, as described in Figure 4b, equation 11 needs to be inverted. To ensure stability of the inverse filter, which may become unstable due to zeros, Z_k, located outside the unit circle, the filter form in equation 11 must be transformed into a minimum-phase representation, denoted by H^{ϵ}_{min}, as outlined in [5]. This minimum-phase filter accurately models the strain-force transfer function of the cutting tool, enabling the estimation of the force acting on the tool tip using strain response data.

Furthermore, to estimate the tool tip displacement using the predicted force, the displacement-force transfer function of the cutting tool is represented by equation 12, as described in [16].

$$H^{d}_{qq}(s) = \frac{W_q(s)}{F_q(s)} = \sum_{r=1}^{N} \frac{\mathbb{R}_{qqr}}{s - \lambda_r} + \frac{\mathbb{R}^{*}_{qqr}}{s - \lambda^{*}_r} \tag{12}$$

$$\mathbb{R}_{qqr}, \mathbb{R}^{*}_{qqr} = \mp j \frac{\phi_{qr} \phi_{qr}}{2 \omega_{dr} m_r} \tag{13}$$

where W_q refers to the Laplace transformed transversal displacement at the tool tip, as demonstrated in Figure 3. The individual displacement mode shapes, ϕ_{qr}, are expressed by equation 5. The other parameters in this model have been obtained in previous steps.

To effectively calculate the displacement from predicted force data, the displacement-force transfer function must also be transformed into digital filter form through equation 11. These considerations and models form the basis of the method to accurately estimate force acting on the cutting tool and tool tip displacement using the measured data solely from the strain sensor.

Experimental Verification and Results

The experimental test setup, for method validation, is shown in Figure 6. The complete test structure was fixed on a rigid sprung steel module. The cutting tool equipped with a piezoelectric strain sensor used to measure strain response near the tool clamping where the tool experiences the highest strain level. The impulse hammer, equipped with the force sensor, was used to excite the cutting tool and measure the force as a reference. Additionally, an accelerometer was mounted at the tool tip to measure the acceleration data, used to validate the displacement estimation. The equipment used in the test is listed in Table 2.

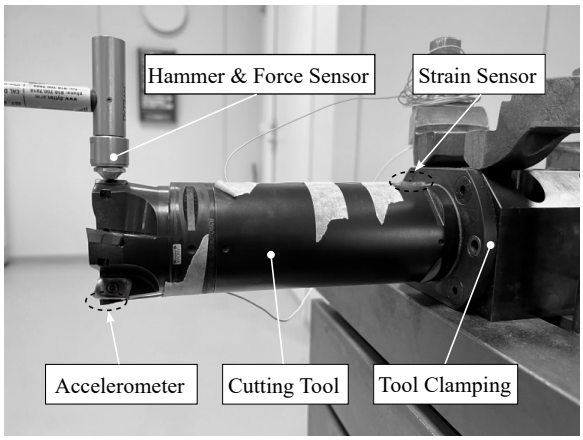

Fig. 6 An illustration of the experimental setup in the lab.

Table 2 Experiment equipment.

Equipment	Model
Impulse hammer	Dytran 5800B4
ICP Strain sensor	PCB 740M04
Accelerometer	Dytran 3224A1
Voltage Input Module	NI 9234

The analytical model was updated using the extracted parameters in terms of first resonance frequency ($\omega_{m1} = 784$ Hz) and corresponding damping ratio ($\zeta_1 = 0.95$ %) obtained from the measured strain response to improve the model correlation to the strain response. The comparison between the strain FRFs from updated model, H^{ϵ}_{ana}, and the measurement ,H^{ϵ}_{mea}, is shown in Figure 7. Good similarity confirms the updated model accurately captures the real setup configuration. The strain FRF of the minimum-phase filter, H^{ϵ}_{min}, is also similar to the measurement.

To validate accuracy of transformation between the analytical model, H^{ϵ}_{ana}, and its minimum-phase digital filter form, H^{ϵ}_{min}, a combined strain FRF is introduced by equation 14 and shown in Figure 8.

$$H^{\epsilon}_{com} = H^{\epsilon}_{ana} \cdot (H^{\epsilon}_{min})^{-1} \tag{14}$$

The magnitude of the combined strain FRF remains unity confirming good alignment of the transformation from the analytical model to its minimum-phase filter form. Furthermore, to examine the frequency limitation of the model for force estimation, the phase response $\Theta(\omega)$ of the combined strain FRF ,H^{ϵ}_{com}, is presented in Figure 8. The phase remains approximately linear up to 2300 Hz indicating a frequency limitation of the model [10].

To avoid amplitude distortions caused by the nonlinear phase response, a low-pass filter with a cutoff frequency of 2300 Hz needs to be applied to the estimated forces using inverse filtered strain response data. Additionally, the linear phase

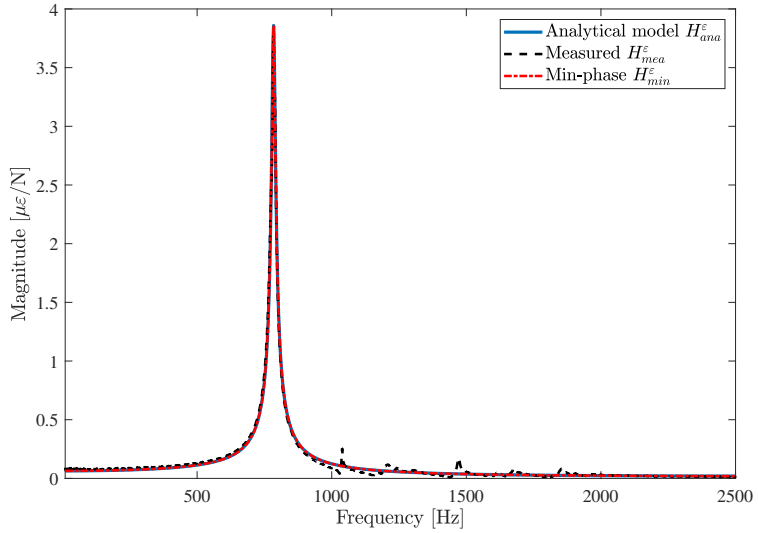

Fig. 7 comparison of the strain FRFs from the analytical model after model updating H^{ϵ}_{ana}, the measurement H^{ϵ}_{mea}, and the minimum phase transformation H^{ϵ}_{min}.

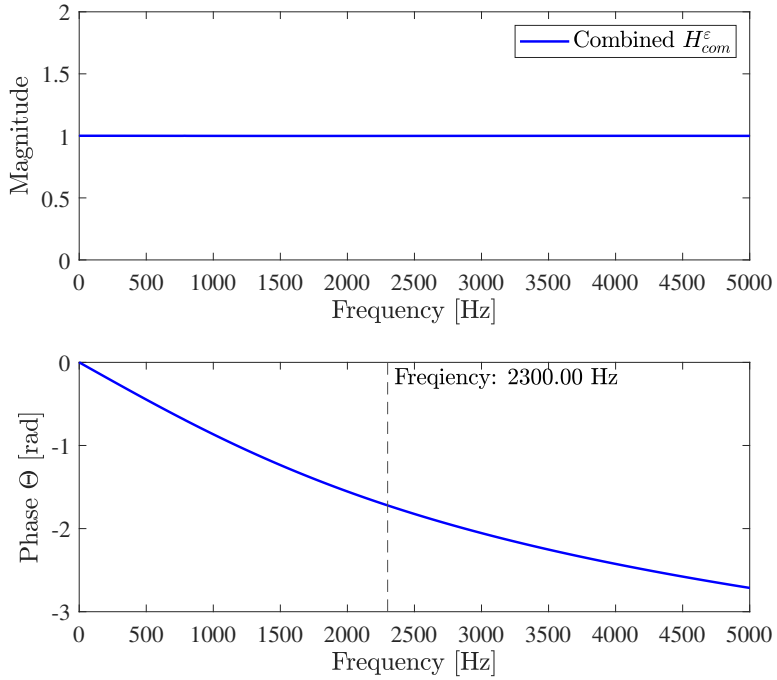

Fig. 8 Illustration of the combined strain FRF, H^{ϵ}_{com}, by the strain FRF of analytical model, H^{ϵ}_{ana}, multiplying the strain FRF of inverse minimum-phase filter, $(H^{\epsilon}_{min})^{-1}$.

response of the transfer function corresponds to a delay in the time domain. The time delay can be calculated based on the linear phase response by equation 15 [17]. In Figure 8, the time delay is approximately 0.126 ms.

$$D(\omega) \triangleq -\frac{d}{d\omega}\Theta(\omega) \tag{15}$$

The results of estimated and measured impact forces are shown in Figure 9. The test result shows good agreement between the measured and predicted impact forces, highlighting the capability of the proposed method for estimating forces acting on the tool tip based on measured strain response data.

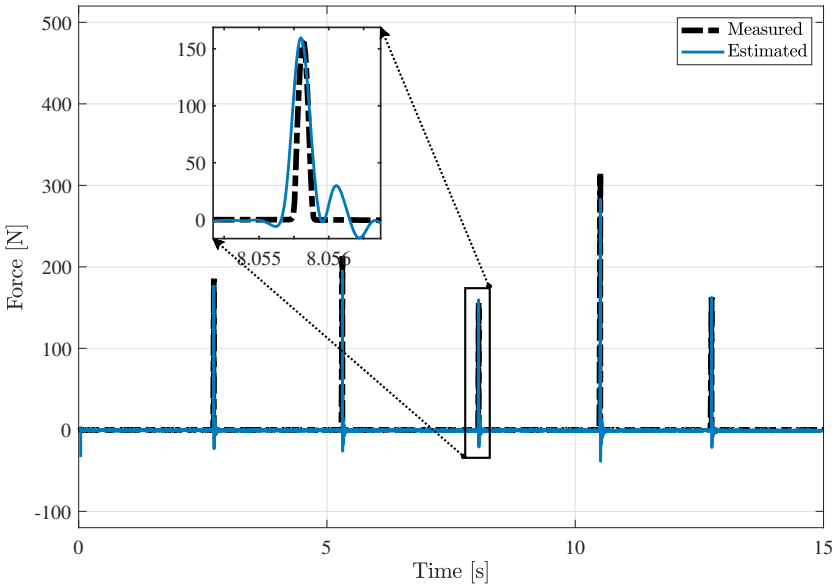

Fig. 9 Comparison between measured and estimated impact forces.

Using the estimated force as input to the displacement-force model, the tool tip displacement is calculated. To obtain a reliable tool tip displacement estimation as reference for validation, an approach is presented in [18]. In this method, the acceleration FRF of the experimental setup is estimated based on the impulse hammer and accelerometer measurement. The measured acceleration FRF is then converted to displacement. A state-space model is then fitted to the measured displacement FRF using MATLAB's system identification toolbox[19], Figure 10.

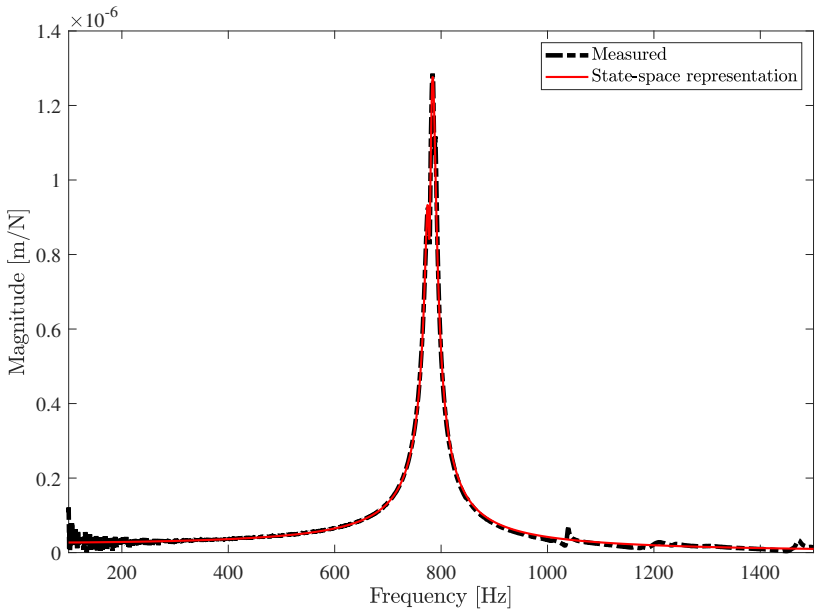

Fig. 10 Comparison between the measured displacement FRF and the state-space model.

The comparison between the displacement obtained from the proposed method based on strain measurements and inverse filtering and the validation approach is shown in Figure 11. The results shows good similarity, indicating that the tool tip displacement can be accurately estimated based on the measured strain by the proposed method.

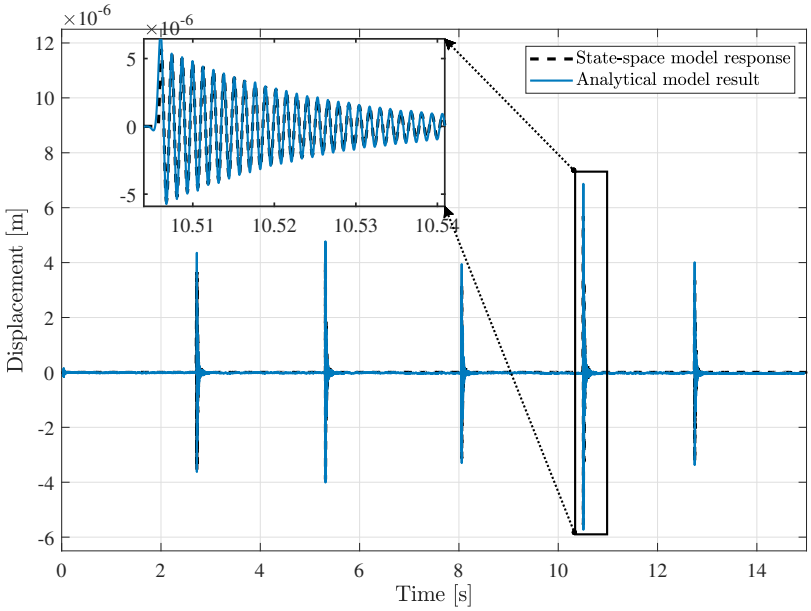

Fig. 11 Comparison between the results of transient displacement at cutting tool tip from state-space model response and analytical model estimation.

Conclusion

A method to estimate the force and displacement based on strain measurements has been tested on a physical cutting tool. The method uses inverse filtering of measured strain to estimate the applied force. The estimated force is then used together with a model of the cutting tool to estimate the displacement at the tool-tip. Both these steps relies on having an accurate model representing the cutting tool under the given configuration.

The feasibility of calibrating the model to align with the real cutting tool configurations using only response data have been successfully validated. The limited need for measurement data in combination with fast model updating represents a significant advantage for practical implementation, as it enables possibility for in-field calibration without the need for complex setups involving modal hammers or shakers.

Further, the results indicate that the proposed method is able to accurately estimate the dynamic forces and tool tip displacements. The strong agreement between the estimated and measured results demonstrates the model's effectiveness in eliminating unwanted dynamic effects of the cutting tool across a wide frequency range.

Overall, this study highlights the potential for accurately predicting dynamic forces and tool tip displacements through the use of strain sensors in cutting tools, facilitating improved performance monitoring and optimization in machining operations.

Acknowledgments The authors wish to acknowledge the financial support provided by AB Sandvik Coromant.

References

1. Brinksmeier, E., Heinzel, C., Wilkens, A., Lang, W., and Seedorf, T. "Monitoring of machining processes using sensor equipped tools". *Advanced Engineering Materials*, 12(7):641–645 (2010)
2. Korkmaz, M.E., Gupta, M.K., Li, Z., Krolczyk, G.M., Kuntoğlu, M., Binali, R., Yaşar, N., and Pimenov, D.Y. "Indirect monitoring of machining characteristics via advanced sensor systems: A critical review". *The International Journal of Advanced Manufacturing Technology*, 120(11-12):7043–7078 (2022)
3. Bhuiyan, M. and Choudhury, I. "13.22—review of sensor applications in tool condition monitoring in machining". *Comprehensive Materials Processing*, 13:539–569 (2014)
4. Kammer, D.C. "Estimation of structural response using remote sensor locations". *Journal of guidance, control, and dynamics*, 20(3):501–508 (1997)
5. Magnevall, M., Lundblad, M., Ahlin, K., and Broman, G. "High frequency measurements of cutting forces in milling by inverse filtering". *Machining science and technology*, 16(4):487–500 (2012)

6. Castro, L.R., Viéville, P., and Lipinski, P. "Correction of dynamic effects on force measurements made with piezoelectric dynamometers". *International Journal of Machine Tools and Manufacture*, 46(14):1707–1715 (2006)
7. Tounsi, N. and Otho, A. "Identification of machine–tool–workpiece system dynamics". *International Journal of Machine Tools and Manufacture*, 40(9):1367–1384 (2000)
8. Yaldız, S. and Ünsaçar, F. "Design, development and testing of a turning dynamometer for cutting force measurement". *Materials & design*, 27(10):839–846 (2006)
9. Östling, D., Jensen, T., Tjomsland, M., Standal, O., and Mugaas, T. "Cutting process monitoring with an instrumented boring bar measuring cutting force and vibration". *Procedia CIRP*, 77:235–238 (2018)
10. W. Peng, M. Magnevall, A. Liljerehn and D. Östling. "Cutting force estimation in metal cutting tools: a study on a sensor-equipped cantilever beam". *Presented at ISMA2024 Conference on Noise and Vibration Engineering* (2024)
11. Thomson, W.T. "Theory of vibration with applications". *NASA STI/Recon Technical Report A*, 93:39794 (1993)
12. Aenlle, M., Juul, M., and Brincker, R. "Modal mass and length of mode shapes in structural dynamics". *Shock and Vibration*, 2020:1–16 (2020)
13. Nishiwaki, N., Masuko, M., Ito, Y., and Okumura, I. "A study on damping capacity of a jointed cantilever beam: 1st report; experimental results". *Bulletin of JSME*, 21(153):524–531 (1978)
14. Lamarque, C.H., Pernot, S., and Cuer, A. "Damping identification in multi-degree-of-freedom systems via a wavelet-logarithmic decrement—part 1: theory". *Journal of Sound and Vibration*, 235(3):361–374 (2000)
15. Şafak, E. "Identification of linear structures using discrete-time filters". *Journal of Structural Engineering*, 117(10):3064–3085 (1991)
16. Brandt, A. *Noise and vibration analysis: signal analysis and experimental procedures*. John Wiley & Sons (2023)
17. Smith, J.O. *Introduction to digital filters: with audio applications*, volume 2. Julius Smith (2007)
18. Gindy, M., Vaccaro, R., Nassif, H., and Velde, J. "A state-space approach for deriving bridge displacement from acceleration". *Computer-Aided Civil and Infrastructure Engineering*, 23(4):281–290 (2008)
19. Johansson, R., Robertsson, A., Nilsson, K., and Verhaegen, M. "State-space system identification of robot manipulator dynamics". *Mechatronics*, 10(3):403–418 (2000)